

COMPARISON OF DISPLACEMENT VERSUS NATURAL VARIABLES FOR THE NUMERICAL SIMULATION OF A STRING PENDULUM

Poth W., Matzl M., Auzinger W., Steindl A. and Troger H.

Institut für Mechanik
Technische Universität Wien
A-1040 Wien, AUSTRIA

ABSTRACT

Simulation of the dynamic behaviour of tethered satellite systems requires the numerical solution of a system of coupled nonlinear partial and ordinary differential equations. Due to the design of tethered satellite systems this set of equations of motion is a stiff system. To integrate this system of equations of motion numerically creates a number of problems. In order to address and solve some of these problems we consider the simpler mechanical model of the string pendulum which, however, displays all relevant features of a tethered satellite system.

In this paper a comparison of two different choices of variables and of various different choices of time integrators is presented in their influence on the efficient and accurate numerical integration of large amplitude motions of the string pendulum. Our results show that for stiff strings a description of the deformation of the string alternative to the usual description by displacements may result in a substantial increase both of accuracy and reduction of computation time. Further the proper choice of the time integrator has great influence as well.

INTRODUCTION

The motivation to do this investigation follows from problems encountered in simulating the equations of motion of tethered satellite systems (Beletsky & Levin (1993), Steiner et al (1995), Wiedermann et al (1999)), that is two or more satellites connected by thin cables in orbit around a planet. Due to several more or less successful flights in orbit around the Earth during the past decade (see the NASA-homepage: <http://www.nasa.gov>) tethered satellite systems (TSS), have gained a lot of interest. By now TSS are a well established new technology for space exploration with great future application potential (Beardsly 1999, Hoyt et al 1999).

Even if simple mechanical models for the TSS are used – typically the cable is modeled as a massive string and the endbodies as massive points or rigid bodies – the equations of motion for large amplitude motions of such systems are a system of coupled nonlinear partial and ordinary differential equations. Since, in addition, practically used tethers, compared to the acting forces, are very stiff concerning their axial extension the equations are stiff in mathematical sense (Hairer & Wanner 1991). This means that

motions in the system dynamics are present which evolve on different time scales. For a TSS this is easy to understand since it is obvious that its motion can be split into very fast oscillations in axial direction of the tether and into two comparably slow oscillations. One is the oscillation of the tether in the direction transversal to its tangent. The other, is the overall motion of the whole system, which is also a relatively slow oscillation.

For the simpler model of the string pendulum which we consider in this paper, qualitatively, the same situation exists. The different motions which evolve on different time scales are shown in Fig. 1. The two left sketches show the overall pendulum swing and the transversal string oscillation which represent the slow motions, whereas in the third sketch to the right the fast axial oscillation is shown. Already in Beletsky & Levin (1993), Hairer & Wanner (1991) and Kuhn (1995) an alternative formula-

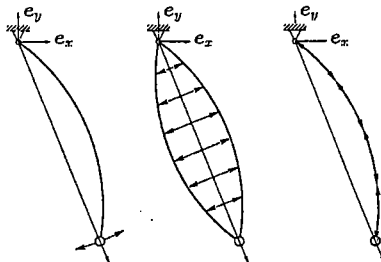


Figure 1: Separation of the oscillation of a string pendulum into slow and fast motions.

tion of the equations of motion for such problems is proposed. Instead of describing the deformation of the string by its displacement components as variables the orientation of the tangent vector t to the deformed tether and the strain ϵ of the tether (or the elongation η) are used. However to the best knowledge of the authors no investigations exist where under same conditions a fair comparison of the numerical efficiency of these two formulations is given. To integrate a stiff system of nonlinear differential equations numerically stable in time, implicit integration schemes must be used in order to achieve reliable and accurate results. Here also a great number of different methods is available. Two goals should be achieved with this paper:

- To compare the influence of the formulation of the equations of motion of the string pendulum by two different sets of variables on the numerical accuracy and efficiency.
- To compare several implicit time integrators concerning speed of integration provided they perform the task.

MECHANICAL MODEL AND EQUATIONS OF MOTION

We consider the string pendulum shown in Fig.2 consisting of a massive continuous flexible viscoelastic string which carries at its end a mass point. The string is without bending and torsional stiffness and of constant length l . To derive the geometric relations we have to distinguish between unstrained arclength s , which is considered as a material coordinate and the strained or actual arclength \hat{s} . In the

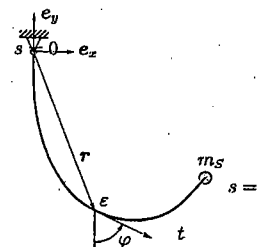


Figure 2: Mechanical model of the string pendulum carrying an end mass m_s

formulation given below the unstrained arclength s with $0 \leq s \leq l$ is used, where l is the length of the string. $()'$ denotes the derivative with respect to the unstrained arclength s . For the strain ϵ and the tangent vector t we obtain

$$\epsilon = \frac{d\hat{s} - ds}{ds} = \eta - 1 = \|\mathbf{r}'\| - 1, \quad \mathbf{t} = \frac{\partial \mathbf{r}}{\partial \hat{s}} = \mathbf{r}' \frac{1}{\eta}, \quad (1)$$

where η is the elongation. In a geometrically exact, large displacement, but small strain description of the deformation we stipulate as constitutive relation for the string the linear Kelvin-Voigt law of viscoelasticity

$$N = EA(\epsilon + \alpha \dot{\epsilon}), \quad (2)$$

relating the axial force N in the string with the strain ϵ , where EA is the axial stiffness and α a dissipation constant. $()'$ denotes the derivative with respect to time t .

Displacement components used as variables

The vector $\mathbf{r}(s, t)$ to a point of the string is represented by its components in the (e_x, e_y) frame. The field equation of motion for the string is given by (Beletsky & Levin)

$$\ddot{\mathbf{r}} - \frac{1}{\mu} (N \mathbf{t})' - \mathbf{g} = \mathbf{0}, \quad (3)$$

where \mathbf{g} is the gravitational acceleration and the string mass per unit unstrained length is denoted by μ . The boundary conditions at the pivot is $\mathbf{r}(0, t) = \mathbf{0}$ and at the mass point it is given by $\mathbf{r}(l, t) = \mathbf{r}_s(t)$ where $\mathbf{r}_s(t)$ follows from the equation of motion

$$\ddot{\mathbf{r}}_s + \frac{1}{m_s} N(l) \mathbf{t}(l) - \mathbf{g} = \mathbf{0}, \quad (4)$$

of the end mass.

Natural string variables: $\epsilon - t$

Starting from (1), alternatively to the displacement components, the position vector $\mathbf{r}(s, t)$ can be represented by the strain ϵ and the tangent vector t in the form

$$\mathbf{r}(s, t) = \int_0^s (\epsilon + 1) \mathbf{t} d\sigma. \quad (5)$$

Taking the derivatives

$$r' = (\varepsilon + 1)t, \quad r'' = [(\varepsilon + 1)t]', \quad \dot{r}' = [(\varepsilon + 1)t]', \quad \ddot{r}' = [(\varepsilon + 1)t]''$$

we calculate

$$\int_s^l \ddot{r} \, d\sigma = \dot{r}_\sigma \Big|_s^l - \int_s^l \dot{r}' \, d\sigma = \int_0^l G[(\varepsilon + 1)t]'' \, d\sigma, \quad (6)$$

where $G = l - \max(s, \sigma)$ is a modified Green's function. Relation (6) follows from an integration by parts of the left hand side and taking into account that $r(0) = 0$ and $r(l) = r_S$. With (6) we can write Newton's law for the part of the string from s to l in the form

$$\int_0^l G[(\varepsilon + 1)t]'' \, d\sigma - g(l - s) - \frac{1}{\mu} (N(l)t(l) - N(s)t(s)) = 0, \quad (7)$$

which results in the implicit form of the equation of motion of the string. In order to include the boundary condition at the end mass m_S into the equation we substitute for the string force at $s = l$ in (7) the following expression

$$N(l)t(l) = m_S(g - \ddot{r}_S) = m_S g - m_S \int_0^l [(\varepsilon + 1)t]'' \, d\sigma, \quad (8)$$

which follows from (4). Here use is made of

$$\int_0^l [(\varepsilon + 1)t]'' \, d\sigma - \ddot{r}_S = 0, \quad (9)$$

which follows from (5). Now (7) takes the form

$$\int_0^l \bar{G}[(\varepsilon + 1)t]'' \, d\sigma - \left(\frac{m_S}{\mu} + l - s\right)g + \frac{1}{\mu} N(s)t(s) = 0 \quad (10)$$

with the generalized Green's function

$$\bar{G} = \frac{m_S}{\mu} + l - \max(s, \sigma)$$

The advantage of equation (10) is that the boundary condition at the end mass is included.

DISCRETIZATION OF THE EQUATIONS OF MOTION IN SPACE

The discretization in space of the partial differential equations is performed by Finite Differences.

Displacement components used as variables

In the case where the deformation is represented by the displacement components we use one-sided difference quotients for the following quantities

$$\Delta^+ r_i = \frac{k}{l} (r_{i+1} - r_i), \quad \Delta^- r_i = \frac{k}{l} (r_i - r_{i-1}) \quad (11)$$

$$\varepsilon_i^+ = \|\Delta^+ r_i\| - 1, \quad \varepsilon_i^- = \|\Delta^- r_i\| - 1, \quad \dot{\varepsilon}_i^+ = \frac{\Delta^+ \dot{r}_i \cdot \Delta^+ r_i}{\varepsilon_i^+ + 1}, \quad \dot{\varepsilon}_i^- = \frac{\Delta^- \dot{r}_i \cdot \Delta^- r_i}{\varepsilon_i^- + 1} \quad (12)$$

$$t_i^+ = \frac{\Delta^+ r_i}{\varepsilon_i^+ + 1}, \quad t_i^- = \frac{\Delta^- r_i}{\varepsilon_i^- + 1}, \quad N_i^+ = EA(\varepsilon_i^+ + \alpha \dot{\varepsilon}_i^+), \quad N_i^- = EA(\varepsilon_i^- + \alpha \dot{\varepsilon}_i^-). \quad (1)$$

Here is k the number of elements into which the string length l is divided. We note that the discretization of the strain ε is a delicate point and can be done in various different ways, which may strongly influence the numerical results obtained (Poth 1999). In this paper the choice is made that the respective term the equations of motion $(N_i t_i)'$ will be represented by $k(N_i^+ t_i^+ - N_i^- t_i^-)$. The discretization of the field equation (3) then yields a set of ordinary differential equations of the form

$$\ddot{r}_i - \frac{k}{\mu l} (N_i^+ t_i^+ - N_i^- t_i^-) - g = 0 \quad i = 1, 2, \dots, k. \quad (1)$$

Natural string variables: ε, t

The discretization of (10) results in

$$Mx + z = 0, \quad (1)$$

where the vectors are given by

$$x_i = [(\varepsilon_i + 1)t_i]'', \quad z_i = -l\left(\frac{m_S}{\mu} + 1 - \frac{i}{k}\right)g + \frac{1}{\mu} N_i t_i. \quad (1)$$

In the calculation of the matrix M integrals must be evaluated. This is done using the trapezoidal rule. The following weight factors are used in the integration

$$w(j) = \frac{l}{2k} \begin{cases} 1 & j = 0, k \\ 2 & \text{otherwise.} \end{cases}$$

For the matrix M and its inverse we obtain with $a = k \frac{m_S}{\mu}$

$$M = \frac{l^2}{2k^2} \begin{pmatrix} a+k & 2(a+k-1) & 2(a+k-2) & \dots & a \\ (a+k-1) & 2(a+k-1) & 2(a+k-2) & \dots & a \\ (a+k-2) & 2(a+k-2) & 2(a+k-2) & \dots & a \\ \vdots & \vdots & \vdots & \ddots & \vdots \\ a & 2a & 2a & \dots & a \end{pmatrix}, \quad M^{-1} = \frac{k^2}{l^2} \begin{pmatrix} 2 & -2 & & & \\ -1 & 2 & -1 & & \\ & -1 & 2 & -1 & \\ & & \ddots & \ddots & \ddots \\ & & & -1 & 2 & -1 \\ & & & & -1 & 2 & -1 \\ & & & & & -2 & 2(a+1) \end{pmatrix}. \quad (17)$$

The following set of discretized equations of motion is obtained. Inside the domain for $i \in [1, k-1]$ one has

$$[(\varepsilon_i + 1)t_i]'' - \frac{k^2}{\mu l^2} (N_{i+1} t_{i+1} - 2N_i t_i + N_{i-1} t_{i-1}) = 0 \quad (18)$$

and at the boundaries

$$[(\varepsilon_0 + 1)t_0]'' - 2\frac{k}{l}g - 2\frac{k^2}{\mu l^2} (N_1 t_1 - N_0 t_0) = 0 \quad (19)$$

$$[(\varepsilon_k + 1)t_k]'' + 2\frac{k^2}{\mu l^2} (N_k t_k - N_{k-1} t_{k-1}) + 2\frac{k}{m_S l} N_k t_k = 0.$$

We note that the boundary conditions are taken care of in these equations. At the boundary we obtain differential equation. An alternative derivation of the boundary conditions is given in Beletsky & Levit (1993). However, this results in an algebraic equation of the boundary. It turned out that this is no convenient from a numerical point of view.

Representation of the tangent vector

The tangent vector can be represented in various ways. Here, where we will consider only planar oscillations of the string pendulum, the best choice would be by the angle φ as shown in Fig.2. However, for three-dimensional motions, angles are not the best choice because in certain positions singularities occur. In order to make the numerical results obtained below relevant also for the three-dimensional case we use cartesian components as parametrization of the tangent vector which works fine also in three dimensions. The highest derivative in t reads

$$((\varepsilon_i + 1)t_i)'' = \ddot{\varepsilon}_i t_i + 2\dot{\varepsilon}_i \dot{t}_i + (\varepsilon_i + 1)\ddot{t}_i. \quad (20)$$

For its calculation the tangent vector and the constraint condition are

$$t_i = \begin{pmatrix} t_{1i} \\ t_{2i} \end{pmatrix}, \quad \frac{1}{2}(t_i^T t_i - 1) = 0. \quad (21)$$

Adding the second derivative of the constraint to (20) results into the following expression

$$\begin{pmatrix} (\varepsilon_i + 1)t_i \\ \frac{1}{2}(t_i^T t_i - 1) \end{pmatrix}'' = \begin{pmatrix} \varepsilon_i + 1 & 0 & t_{1i} \\ 0 & \varepsilon_i + 1 & t_{2i} \\ t_{1i} & t_{2i} & 0 \end{pmatrix} \begin{pmatrix} \ddot{t}_{1i} \\ \ddot{t}_{2i} \\ \ddot{\varepsilon}_i \end{pmatrix} + \begin{pmatrix} 2\dot{\varepsilon}_i \dot{t}_{1i} \\ 2\dot{\varepsilon}_i \dot{t}_{2i} \\ \dot{t}_{1i}^2 + \dot{t}_{2i}^2 \end{pmatrix}. \quad (22)$$

Denoting the matrix in front of the second derivatives in (22) by A_i , then its determinant is given by $\det(A_i) = -(\varepsilon_i + 1)^2$ and its inverse by

$$A_i^{-1} = \frac{1}{\varepsilon_i + 1} \begin{pmatrix} t_{2i}^2 & -t_{1i}t_{2i} & (\varepsilon_i + 1)t_{1i} \\ -t_{1i}t_{2i} & t_{1i}^2 & (\varepsilon_i + 1)t_{2i} \\ (\varepsilon_i + 1)t_{1i} & (\varepsilon_i + 1)t_{2i} & -(\varepsilon_i + 1)^2 \end{pmatrix}. \quad (23)$$

Multiplying the right hand side of (22) with (23) we see that a separation in equations in slow and fast variables is obtained, concerning the highest order of the derivative of the variables in t .

TIME INTEGRATION OF THE STIFF SYSTEM

For the numerically stable integration in time of the set of ordinary differential equations (18) and (19) which are a stiff system in the mathematical sense, implicit methods must be used. An important measure of an used algorithm is its order of consistency p , which indicates with which power h^p of the discretization h the discretization error tends to zero for $h \rightarrow 0$. Another characteristic feature is the number of grid points necessary for the calculation of the next time step. Here one divides into one step and multi-step methods. One step methods are the implicit Euler method, Runge-Kutta methods and the θ -method, which is a combination of the implicit and the explicit Euler method given by θ IEUL + $(1 - \theta)$ EEUL. It contains the explicit ($\theta = 0$) and implicit ($\theta = 1$) Euler method as special cases. For $\theta \geq \frac{1}{2}$ unconditional stability is obtained. However, by using $\theta > \frac{1}{2}$ algorithmic damping is introduced. A popular class of multi-step methods are the BDF-methods (Backward Differentiation Formulae). For the codes listed in Table 1, which fall into these categories, we still can divide into "professional" (LSODI, DASSL, DASPK and RADAU) and "semi-professional" (NEWM, IEUL and THETA) methods.

The professional codes LSODI, DASSL, DASPK and RADAU possess automatic stepsize-control and order-strategy while NEWM, IEUL and THETA use fixed stepsize. Therefore, the error-tolerances in the numerical experiments do not affect both the accuracy and computing time of the latter methods. Thus the accuracy of NEWM, IEUL and THETA is only controlled by the accuracy of the approximate solution of the nonlinear algebraic equations which is determined by the tolerance for Newton's method.

name	method	type of method	order	DAE solver	year
LSODI	BDF	multistep	≤ 5	yes	1987
DASSL	BDF	multistep	≤ 5	yes	1983-91
DASPK	BDF	multistep	≤ 5	yes	1985-95
RADAU	impl. Runge-Kutta	one-step	5, 9, 13	yes	1998
NEWM	Newmark	two-step	1, 2	no	1959
IEUL	impl. Euler	one-step	1	no	-
THETA	θ -method	one-step	1, 2	no	-

Table 1: Various implicit time integrators applied for the numerical integration

NUMERICAL RESULTS

Comparison of the numerical efficiency for the two different sets of variables

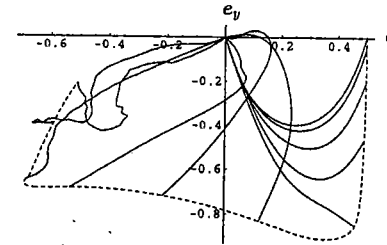


Figure 3: Motion of the visco-elastic string pendulum ($EA = 10^6$) from the initial configuration in the upper right corner to the left, using the displacement variables.

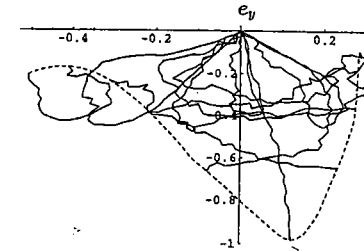


Figure 4: Continuation of the motion of Fig. 3 from the left configuration to the right using the displacement variables.

In the comparison of the two different formulations besides speed of integration also accuracy and the ability to continue the integration for a long time interval was important. The second point means that especially in those phases of the motion of the string pendulum when the string is not under tension the string becomes slack which results in configurations that caused some of the programs to stop the integration. Here it turned out that the formulation in natural variables was much better than the one in displacement variables. This fact is also clearly visible from Figures 3 to 6, where for the natural variables a smoother configuration of the string is obtained than for the displacement variables. The difference in CPU-time for the different formulations is clearly visible from Fig.9, where for the natural string coordinates the representation of the tangent vector, besides by its cartesian components, also the angle φ is given. In this latter case automatically the constraint equation given in (21) is satisfied, hence, this calculation is more time-efficient than the representation by the cartesian components of the tangent vector which, however, usually is used in three dimensions. For the CPU time comparison we scaled such that the fastest integrator (DASSL) and the best formulation (ε, φ) for the string stiffne

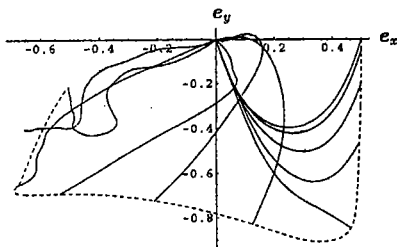


Figure 5: Motion of the visco-elastic string pendulum ($EA = 10^6$) from the initial configuration in the upper right corner to the left using the natural variables ϵ, t .

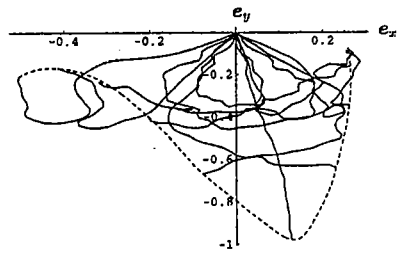


Figure 6: Continuation of the motion of Fig.5 from the left configuration to the right

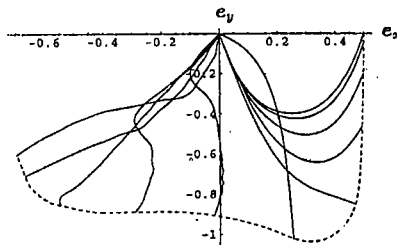


Figure 7: Motion of the visco-elastic string pendulum ($EA = 10^4$) from the initial configuration in the upper right corner to the left using the natural variables ϵ, t .

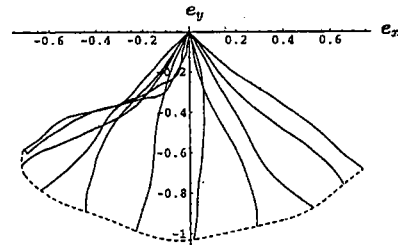


Figure 8: Continuation of the motion of Fig.7 from the left configuration to the right

$EA = 10^4$ result in $CPU = 1$. For all results shown the number of elements in the Finite Difference discretization was set to $k = 40$. Our results show that the simulation time increases approximately with the square of the number of elements. For a comparison we also show the pendulum forth and back swing for a relatively soft string in Figs.7 and 8. Since no difference can be seen by eye inspection for the two sets of variables we only give the results of the formulation in natural variables.

Comparison of various different time integrators

The comparison of the efficiency of various time integrators is given in Fig.10. The following parameters are used: time stepsize: 0.005 (in the Figures the time difference between subsequent configurations is $\Delta t = 0.1$); number of steps: 400; error tolerance for absolute and relative error test: 10^{-7} ; parameter for the θ -method: $\theta = \frac{1}{2}$; parameter for Newmark's method: $\gamma = \frac{1}{2}, \beta = \frac{1}{4}$; tolerance for Newton's method: 10^{-7} . That the semi professional methods IEUL, NEWM and THETA are per-

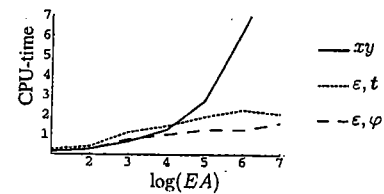


Figure 9: CPU-time as a function of the string stiffness EA for three formulations: Displacement variables, ϵ, t and ϵ, φ . As time integrator DASSL is used

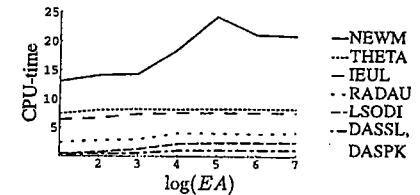


Figure 10: CPU-time as a function of the string stiffness EA for seven different time integrators: DASSL, DASP, LSODI, RADAU, IEUL, THET and NEWM

forming not as well as the professional methods can be explained by the fact that the semi-professional methods are without step size control and hence do not automatically adapt the step size.

Fig.10 shows that the BDF-codes DASSL and DASP are the fastest integrators for soft and stiff strings. The main reason is the moderate effort for solving the nonlinear algebraic equations by Newton's method compared to implicit Runge Kutta methods.

CONCLUSIONS

Two important conclusions can be drawn from the numerical simulation of the large amplitude oscillations of the string pendulum in view of the more complicated problem of simulation of the motion of tethered satellite systems.

If the tether is stiff, without any doubt the formulation in natural coordinates is not only more efficient concerning computation time, but what seems to be of equal significance, also smoother configurations of the string are obtained in case the string becomes slack during the motion of the system. However, we have to remark that the formulation in the natural coordinates is more complicated, especially what concerns the boundary conditions and requires also greater programming efforts.

The second important conclusion is that the used time integration method again may have a strong influence on the result. Here so-called "professional methods" perform much better than so-called "semi-professional" methods which, however, sometimes are more flexible to apply. We refer in this respect to the approach taken by Vu-Quoc & Simo (1987) which is implemented in Wiedermann et al 1999 for tethered satellite systems. In this approach the Newmark method is used for the time integration. What is special with this approach which has also been used in other papers by Simo (e.g. Simo & Vu-Quoc 1986) is that starting from a variational formulation the discretization in time is performed prior to the discretization in space.

ACKNOWLEDGMENTS

Financial support for the authors is gratefully acknowledged to the Austrian Science Foundation (FWF) under project P-13131-MAT and to the European Space Agency (ESA) under the ESTEC/Contract No.12540/97/NL/PA(SC).

REFERENCES

- Beardsley, T.: The Way to go in Space, Scientific American February 1999.
- Beletskii, V. V., Levin, E. M.: Dynamics of Space Tether Systems. AAS 83, 1993.
- Hairer, E., Wanner, G.: Solving Ordinary Differential Equations, II. Stiff and Differential-Algebraic Problems, Springer Verlag, Berlin, Heidelberg 1991.
- Hoyt, R.P., Forward R.L., Nordley, G.D., Uphoff, C.W., Rapid Interplanetary Tether Transport Systems, IAF-99-A.5.10, 50th IAF Congress Amsterdam 1999, 31 pages.
- Kuhn, A.: Numerische Behandlung von "Tethered Satellite Systems" unter besonderer Berücksichtigung längssteifer Verbindungsseile. Ph.D.Thesis TU-Wien, 1995.
- Kuhn, A., Steiner, W., and Troger, H.: Tethered Satellite Systems: Applications, Modelling and Formulation of the Equations of Motion for Very Stiff Tethers. ZAMM 76, 1996, 329-332.
- Misra, A. K., Modi, V.J.: A survey on the dynamics and control of tethered satellite systems AAS 86-246, 1986, 667-719.
- Poth, W.: Vergleich nichtlinearer Formulierungen der Dynamik verkabelter Satelliten. Ph.D.Thesis TU-Wien, 1999.
- Poth, W., Schagerl, M., Steindl, A., Steiner, W., and Troger, H.: "Numerically Efficient Formulation of the Equations of Motion of Tethered Satellite Systems". *Proceedings of IUTAM Symposium on Discretization Methods in Structural Mechanics (H.A.Mung and F.G.Rammerstorfer eds.)* Kluwer Academic Publishers, Dordrecht, 1999, 139-146.
- Simo, J. C. and Vu-Quoc, L.: On the Dynamics in Space of Rods Undergoing Large Motions – A Geometrically Exact Approach. *Computer Methods in Appl. Mech. and Engineering*, vol. 66, 1986, 125-161.
- Steiner, W., Steindl, A., and Troger, H.: Dynamics of a Space Tethered Satellite System with Two Rigid Endbodies. In *Proceedings of the Fourth International Conference on Tethers in Space*. Science and Technology Corporation, Hampton, VA, 1995, 1367-1379.
- Vu-Quoc, L., Simo, J. C.: Dynamics of Earth-Orbiting Flexible Satellites with Multibody Components. *J. Guidance, Control and Dynamics* 10, 1987, 549-558.
- Wiedermann, G., Schagerl, M., Troger, H.: Computation of Force Controlled Deployment and retrieval of a Tethered Satellite System by the Finite Element Method, *Proceedings of ECCM '99 (W.Wunderlich ed.)*, 1999, 410-430.

Nonlinear Dynamics, Chaos, Control and Their Applications to Engineering Sciences. Vol 5: Control and Times Series, 2002. J. M. Balthazar, P. B. Gonçalves, R. M. F. L. R. F. Brasil, I. L. Calda, Rizatto, Editors.
ISBN: 85-900351-5-8

NONLINEAR DYNAMICS AND CONTROL OF A SHUTTLE TANKER

Jessé Rebello de Souza Jr
Helio Mitio Morishita
Claudio Gomes Fernandes
Bruno Jean Jacques Cornet
Department of Naval Architecture and Ocean Engineering
University of São Paulo – Brazil

ABSTRACT

Exploitation of deep-water offshore oil fields like those found in Brazilian basins cannot employ platforms and may require the widespread use of large tankers converted to operate as Flo Production, Storage and Offloading (FPSO) systems. The oil stored in these units has to be periodically transferred to shuttle tankers that remain attached to the FPSO in a tandem configuration during the offloading operation. Clearly, the dynamic behavior of such large floating structures in a – sometimes rough – marine environment is of primary concern. It is particularly important to avoid collisions between the vessels. The dynamics of an FPSO – shuttle tanker tandem system are then investigated here with a view to assessing the need for controlling their motions in the horizontal plane. A first step in this study was the determination of static equilibrium solutions under the combined action of constant current and wind with various angles of incidence and relative magnitudes. Due to the complexity of the mathematical models involved equilibrium equations were solved numerically. It was observed that the system could display several equilibria, most of which are unstable. The system typically settles onto limit cycles in which relative motions pose the risk of collision between the vessels. A control system is then devised based on a nonlinear compensator that supplies the longitudinal force and moment needed. Numerical simulation of the controlled system suggests that the control scheme proposed can be very effective in keeping the vessels safely apart.

INTRODUCTION

FPSO systems have deserved much attention lately because they represent a novel approach to exploiting offshore oil fields in deep water (in excess of 1000m), adapting conventional tanker function as temporary oil storage systems. The use of converted tankers has been dictated by economic reasons, but they present designers with the complex task of devising and implementing adequate positioning systems. This is due to the fact that, unlike a semisubmersible platform, tankers were not originally designed to keep station at sea. The large lateral areas they offer to the action of wind, waves and currents make it technically difficult – and economically impractical – to keep them stationary in deep waters unless they are able to weathervane (at least partially). State-of-the-